Behavior of toluene adsorption on activated carbon nanofibers prepared by electrospinning of a polyacrylonitrile-cellulose acetate blending solution

Young-Wan Ju*,† and Gil-Young Oh

*Departments of Chemical Engineering, College of Engineering, Wonkwang University, Iksan, Jeonbuk 54538, Korea
**JeollaNamdo Institute of Health and Environment, Muan, Jeonnam 58568, Korea

Abstract–Activated carbon nanofibers were prepared with polymer blends that consisted of polyacrylonitrile (PAN) and cellulose acetate (CA), by electrospinning and subsequent thermal treatment. The average fiber diameter of samples was about 200 nm, ranging from 150 to 400 nm. The specific surface area, total pore volume, and micropore volume increased with increasing CA content. As the CA content was increased up to 20%, the pore characteristics for the adsorption performance were enhanced. However, excess CA content (over 30%) was harmful to volatile organic compounds (VOCs) adsorption ability due to changing morphology of the activated carbon nanofibers. The O/C ratio was increased with increasing CA content. However, the O/C ratios of all activated carbon nanofibers prepared with blends represent small values revealing non-polarity of the surface. The adsorption capacities of PC10, PC09, PC08 and PC07 were 65 g/100 g, 66 g/100 g, 72 g/100 g and 67 g/100 g. The blends of the PAN with CA showed better characteristics than those of PAN alone, but apparently there is an appropriate blending ratio (20%) for high-performance of activated carbonaceous materials.

Keywords: Activated Carbon Nanofiber, Electrospinning, Adsorption, Surface Properties, Volatile Organic Compounds

INTRODUCTION

Volatile organic compounds (VOCs) are organic chemicals that have a high vapor pressure and easily form vapor at normal temperature and pressure. The term is generally applied to organic solvents, certain paint additives, aerosol spray can propellants, fuels, petroleum distillates, dry cleaning products and many other industrial and consumer products [1-3]. VOCs are also naturally emitted by a number of plants and trees [4]. Since VOCs are important health and environmental concerns, various studies have focused on ways to control them [5-9]. VOCs can be classified into two groups. One group of VOCs comprises hazardous air pollutants or persistent organic pollutants (POPs), and benzene, dioxin, DDT, etc. can be in this group. The other is for VOCs as photochemical oxidants precursors such as ozone or peroxoacetylnitrate. The latter consists of many kinds of light hydrocarbons, including naphtha, toluene, and ethylene [10,11]. Toluene, in particular, plays an important role in VOCs as photochemical oxidants precursor. Toluene can be removed with special methods, for example, absorption, adsorption, condensation, thermal oxidation, catalytic oxidation and some bio-treatment [12]. Considering the low concentration of toluene, adsorption is one of the techniques which provide better efficiency. The adsorption can be carried out by different adsorbents. Recently, activated carbon fiber (ACF) has shown outstanding performance because of its higher surface area and kinetic properties [1,13-15]. ACFs derived from nitrogen-containing mate-

rial, like PAN, have unique properties after pyrolysis. In the pyrolysis (stabilization, carbonization, activation) process, the nitrogen atoms change the electron property, surface chemistry and structure. The changes eventually have an improved effect on their application [16]. The effects of pyrolysis include the formation of heteroaromatic or cyclic structure, tautomerization, dehydrogenation and radical condensation [17]. Furthermore, PAN-derived radicals take hydrogens from molecules and promote cross-linking, resulting in good structural order [18]. These atomic-level changes can affect the chemical and physical properties of the final products. Activated carbon nanofibers (ACNFs) prepared using an electrospinning technique have smaller fiber diameter, resulting in high specific surface area, small pore size, and better kinetic properties than those of conventional ACF [19-23]. Electrospinning is a technique providing nanofibers in the form of a non-woven web through splitting the charged jet by the applied field of electrostatic potential [24-27]. The narrow micropores have better efficiencies for VOCs adsorption and can be prepared easily from proper activation of electrospun fibers [28]. In previous study, we confirmed the outstanding adsorption capacity of PAN-based activated fiber by electrospinning method owing to appropriate pore diameter and surface chemistry like the atomic ratio of oxygen to carbon (O/C) [29].

The blending of different polymers is a robust method for producing new structural materials from existing ones. Often blending is an attempt to meet both performance and economic targets, by mixing a lower priced polymer with a higher performing one. Changing structure by blending can have a significant impact on the performance, such as the adsorption capacity and adsorption rate [30]. Cellulose acetate (CA), universally recognized as the most important organic ester of cellulose because of its extensive applications in fibers,

†To whom correspondence should be addressed.
E-mail: ywju1978@wku.ac.kr

plastics, and coatings, is prepared by reacting cellulose with acetic acid as a solvent and perchloric acid or sulfuric acid as a catalyst [31]. Cellulose esters are used in miscible blends with polymers due to their ability to form hydrogen bonds through the presence of hydroxyl groups and the carboxyl groups of the ester [32]. Another important advantage of CA is its low cost compared to other polymers, and its annulation structure itself may finally make aromatic structure resulting in higher pore volume and surface area.

In this work, activated carbon nanofibers were prepared by electrospinning with PAN and PAN-CA blending solutions at the various blending ratio. The fabricated activated carbon nanofibers were investigated on their character with various analyses and the adsorption capacity of toluene.

EXPERIMENTAL

PAN and cellulose acetate (CA) of 10 wt% were dissolved in the N, N-dimethylformamide (DMF), respectively. And then two solutions were blended at 9:1, 8:2, 7:3 (PAN:CA) by weight. The blended polymer solution was placed in a 30 ml- syringe with a capillary tip (ID=0.5 mm). A power supply (NT-PS-35K, NTSEE, Korea) with a variable high voltage was used for the electrospinning process. The applied voltage was 20 kV, the distance between the tip and the collector was 18 cm, and the flow rate of the spinning solution was 1 mL/h. The electrospun fibers were stabilized by heating them to 280 °C at a rate of 1 °C/min and holding it at this temperature for 1 h in an air atmosphere. The stabilized fibers were carbonized by heating to 1,000 °C at a rate of 5 °C/min and activated by supplying 30 vol% steam for 30 min in a nitrogen atmosphere at 1,000 °C. In this study, an activated carbon nanofiber prepared with polymer blends at the ratio of 9:1, 8:2 and 7:3 is denoted as PC09, PC08, and PC07, respectively. The activated carbon nanofiber based PAN alone was denoted as a PC10.

Specific surface area, pore diameter distribution, and pore volume of all the samples were analyzed by N_2 adsorption (Micromeritics; ASAP2010, USA) at 77 K in the range of relative pressure (P/Po). The morphology of the fibers was analyzed by field emission scanning electron microscopy (FE-SEM, Hitachi, S-4700, Japan). The weight loss of the electrospun web (sample weight is approximately 6.5 mg) was estimated by thermogravimetric analysis over then temperature interval 313-1,273 K with a heating rate of 5 °C/min under 150 mL/min nitrogen flow. (TGA, Stanton Redcroft, STA1640, England). Surface composition and chemistry were characterized on a MultiLab2000 X-ray photoelectron spectroscopy (V.G. Scientific Ltd. England) using non-monochromatic MgKα radiation energy (1,253.6 eV). An X-ray power of 300 W (15 kV, 20 mA) was used for all analyses under vacuum lower than 10^{-9} Pa. Peak intensities were estimated by calculating the integral of each peak, after smoothing, subtraction of an S-shaped background and fitting the experimental curve to a combination of Gaussian and Lorenztian lines of variable proportion.

To confirm VOCs absorption ability of samples, dynamic breakthrough tests were conducted by flowing standard gas through the adsorption cell. The actual height of the adsorption cell was about 15 mm, the internal diameter was 6 mm, and the experiment of adsorption was carried out at 298 K. The amount of ACNF absorbents was approximately 0.06 g. The 200 ppm toluene contained N2 gas was used for test and gas flow was 180 mL/min. Before the test, the samples were outgassed for 2 h using 60 mL/min nitrogen at 573 K. The toluene standard gas through the absorbent was controlled quantitatively by MFC (mass flow controller), and the amount of toluene adsorption was investigated by gas chromatography.

RESULTS AND DISCUSSION

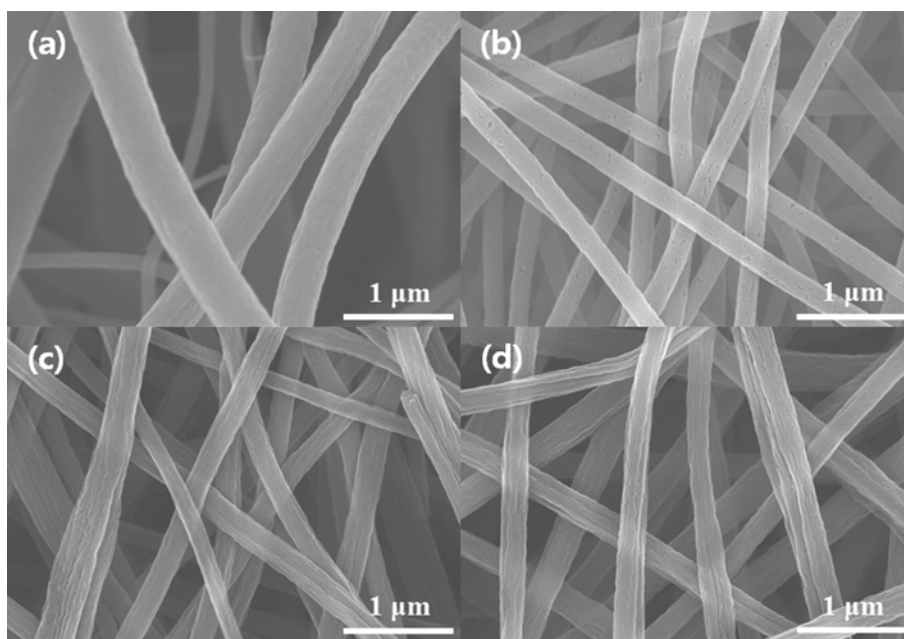Fig. 1 shows the SEM images of the ACNFs (PC10, PC09, PC08,

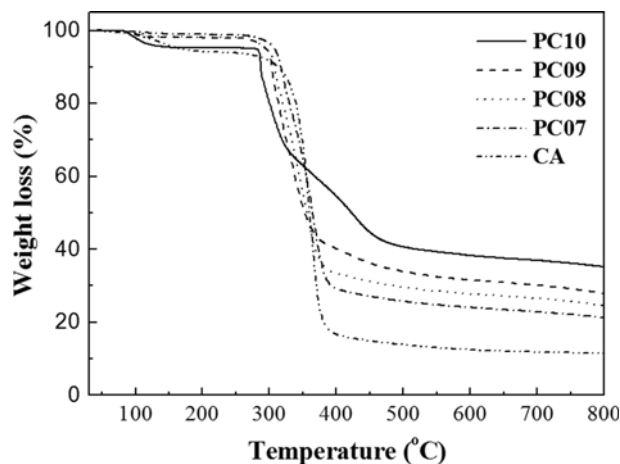**Fig. 1. SEM images of (a) PC10, (b) PC09, (c) PC08 and (d)PC07.**

Fig. 2. TGA profiles of samples.

Table 1. Pore characteristics of the samples

Sample	S.S.A.[a] (m²/g)	T.P.V.[b] (cm³/g)	M.P.V.[c] (cm³/g)	M.P.D.[d] (Å)	A.P.D.[e] (Å)
PC10	1403	0.650	0.505	6.0	40
PC09	1443	0.672	0.519	6.6	45
PC08	1566	0.775	0.606	6.6	51
PC07	1452	0.703	0.453	6.8	61

[a]S.S.A.: specific surface area by BET
[b]T.P.V.: total pore volume
[c]M.P.V.: micropore volume
[d]M.P.D.: median pore diameter (H-K)
[e]A.P.D.: average pore diameter (BJH)

PC07), which have 200 nm average fiber diameter ranging from 150 to 400 nm. The ACNFs prepared with blended polymer solution exhibit rough morphology with wrinkles. The increasing CA content led to a rough surface morphology due to physical processes such as swelling, shrinking or dissolution ascribed to the differences of thermal properties between PAN and CA. The TGA analysis of samples (Fig. 2) revealed that CA was unstable to pyrolyze. It is well known that the thermal degradation pathway of the polymer is influenced by the presence of oxygen groups on materials [33]. Due to increased CA content, the less thermo-stability, CA can be burned-off and result in form valley and halls in the carbonization and activation steps. PC09 having relatively low content of 10% CA lightly changed showing just halls. PC08 having higher content of CA as 20% changed showing warp. As PC07 has the highest CA amount (30%), it was not surprising that this product showed warps and even dislocations.

Fig. 3 shows the nitrogen adsorption/desorption isotherms of PC10, PC09, PC08, and PC07. All isotherms present micropore adsorption behavior (Ty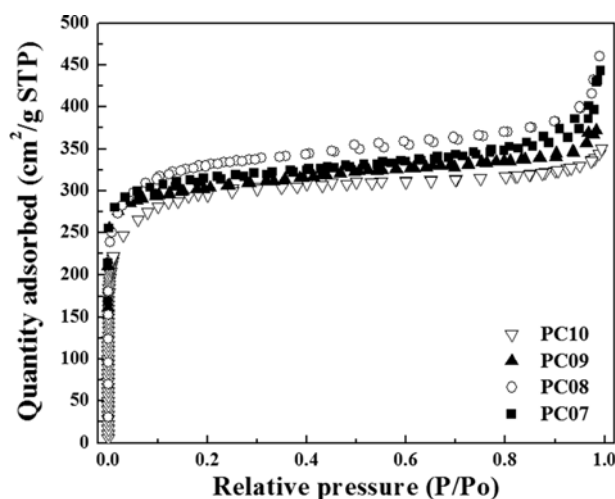pe I), and the process of adsorption is completed at relatively lower pressure (P/Po<0.1). The sharp knees like those isotherms indicate that the samples have a narrow micropore diameter distribution. PC08 and PC07 showed minor hysteresis at the end of the plateau. Therefore, it can be expected that the samples have some mesopore distribution. The nitrogen adsorption capacity of PC08 is higher than other samples. The pore characteristics of the samples are summarized in Table 1. The most developed porosity, corresponded by a BET calculation, PC08 sample had specific surface area of 1,566 m²/g and total pore volume of 0.775 cm³/g. For PC10, the corresponding values were 1,403 m²/g and 0.650 cm³/g, similarly, the corresponding values for PC09 were 1,443 m²/g and 0.672 cm³/g, and for PC07 the values were 1,452 m²/g and 0.703 cm³/g. The specific surface area, total pore volume, and micropore volume increased with increasing CA content up to 20 wt%. However, PC07 showed less specific surface area and total pore volume than PC08, and the sample showed a lower micropore volume than even PC10. The increased CA content is accompanied with the more median pore diameter (H-K) and the more average pore diameter (BJH). As CA content increased to PC08 as 20%, the pore characteristics of the adsorption performance were enhanced. However, an excess of CA (over 30%) content is harmful to the performance of the final product. In con-

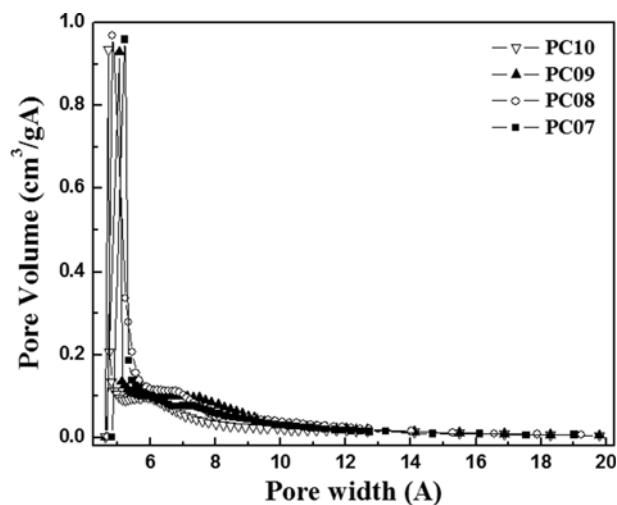Fig. 3. Nitrogen adsorption isotherms (77 K) of samples.

Fig. 4. Micropore volume distribution of samples.

clusion, the PAN-CA blends result in better characteristics, but apparently there is a critical blending ratio for high-performance activated carbonaceous materials. Fig. 4 shows the pore distributions of PC10, PC09, PC08 and PC07 using the Horvath-Kawazoe (H-K, micropore) method. The micropore distribution of all samples is similar and the median micropore diameter of PC10, PC09, PC08 and PC07 are 6.0, 6.6, 6.6 and 6.8 Å, respectively. While the median pore diameter increased with increasing CA content, micro-pore distribution was still narrow (6-7 Å), representing a high specific surface area that can promote a higher toluene adsorption capacity and faster kinetics in the adsorption/desorption process due to the overlap of attractive force of opposite pore walls [32]. The average pore diameters calculated with the Barrett-Joyner-Halenda (BJH) method of PC10, PC09, PC08 and PC07 were 40, 45, 51 and 61 Å, respectively. The average mesopore diameter increased with increasing CA content also. On the other hand, blends were showing a unique pattern in the mesopore distribution (Fig. 5). Unlike PC10, which is pure PAN, blends have higher pore area at a pore diameter of around 35 Å, which can be important in adsorption considering toluene molecular size (106.2 cm^3/mol) [35]. Based on the pore distribution versus surface area and pore volume, at optimum blending ratio (PC08 as 20%), CA admixture resulted in physically positive changes such as swelling and twist by thermal treatment increasing surface area, which can be much more activated by steam. However excessive admixture (PC07)
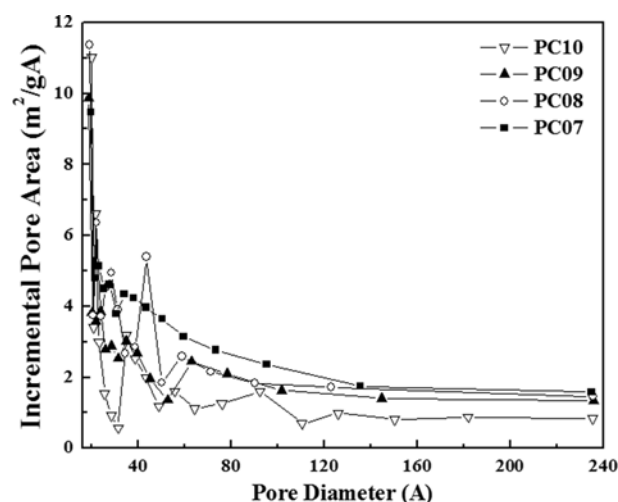

Fig. 5. Mesopore area distribution of samples.

had a bad influence upon the composite, such as the lower surface area and pore volume.

X-ray photoelectron spectroscopy (XPS) was used to determine the elemental composition on the surface of samples. The chemical composition of the carbon surface, especially non-polarity or polarity of its constituents, plays an important role in the toluene
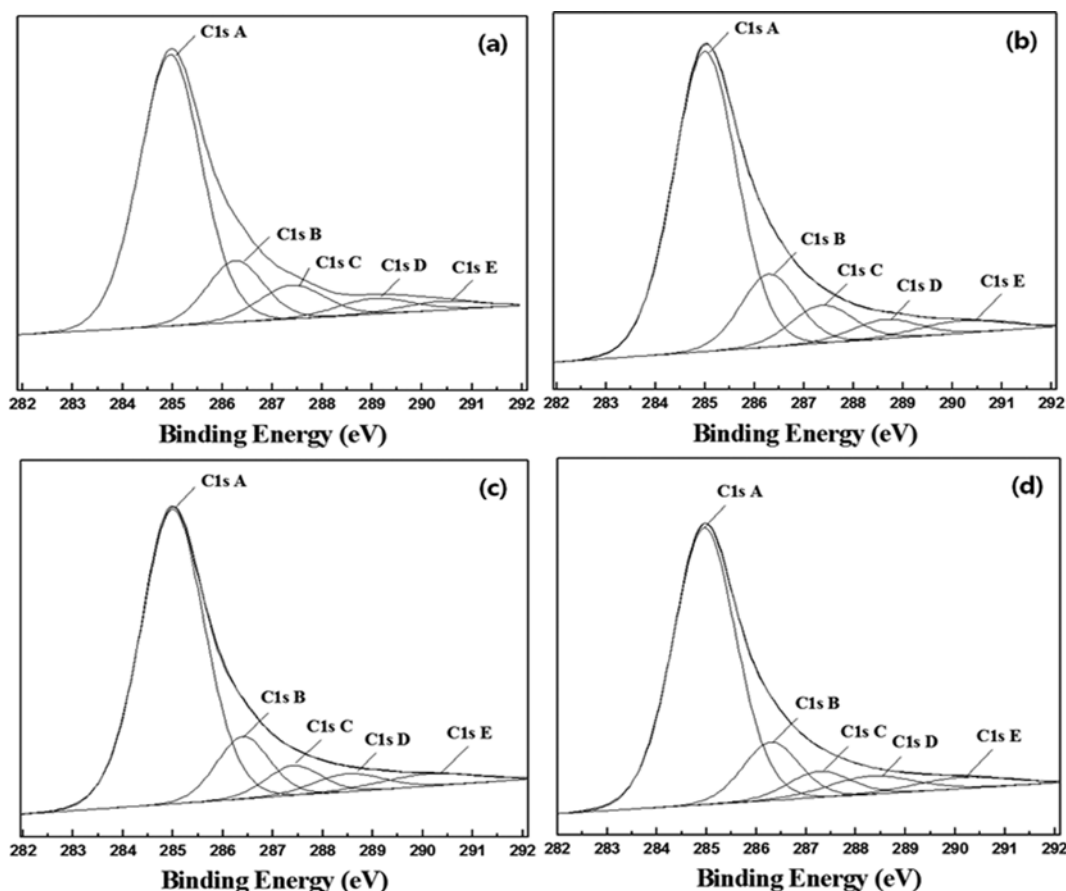

Fig. 6. C1s XPS spectra of (a) PC10, (b) PC09, (c) PC08 and (d) PC07.

**Table 2. Elemental surface composition determined from XPS analysis**

Sample	Total carbon (at%)	Total oxygen (at%)	Total nitrogen (at%)	O/C ratio
PC10	95.64	1.75	2.61	0.018
PC09	95.55	1.91	2.54	0.020
PC08	95.40	2.18	2.42	0.023
PC07	95.39	2.36	2.25	0.025

adsorption mechanism. Oxygen surface groups play an important role in this regard. The XPS C1s spectra for the samples are presented in Fig. 6. The C1s peaks provide the presence of several surface functional groups. To distinguish the complexes, a curve-fitting was conducted. More precisely, the 285.0±0.1 eV is associated with C-C bonds (graphitic carbon), the component at 286.3±0.1 eV with C-O bonds (hydroxyl), the component at 287.3±0.1 eV with C=O bonds (carbonyl) and the component at 288.3±0.2 eV with O=C-O bonds (carboxyl) in carbonates [36,37]. Table 2 represents the O/C atomic ratio obtained from XPS analysis. The carbon, oxygen and nitrogen content of PC10 are 95.64, 1.75 and 2.61 at%, those of PC09 are 95.55, 1.91 and 2.54 at%, those of PC08 are 95.40, 2.18 and 2.42 at% and those of PC07 are 95.39, 2.36 and 2.25 at%. The O/C ratio increased with increasing CA content. Nevertheless, the O/C ratio of blends had small values

representing non-polarity of carbon surface. In general, the oxygen in absorbent surface restricts the adsorption of VOCs like toluene due to the non-polarity of toluene [38,39]. More π-π interaction between the surface of absorbent and toluene leads to higher toluene adsorption capacity.

The XPS N1s spectra for the samples are presented in Fig. 7. Specifically, the 401.20.2 eV is associated with quaternary N, the component at 398.4±0.1 eV with pyridine and the component at 402.3±0.3 eV with oxidized N and the component at 400.1±0.1 eV with pyridone or pyrrole in carbonates. Taking the blending ratio into consideration, nitrogen content in surface had no considerable changes when compared with the amount of nitrogen precursor of PAN. According to the report by Raymundo-Pinero et al., the mixture containing the nitrogen showed content variation after thermal treatment [36]. That is, after stabilization, there was an enrichment of the N species at the surface and, after carbonization, the opposite occurred. So, in this study, there were no N-component ratio changes at the surface of the final product in proportion to nitrogen blending ratio.

Fig. 8 shows the breakthrough curves obtained from toluene adsorption at 200 ppmv toluene concentrations at 25 °C, for PC10, PC09, PC08, and PC07. The breakthrough time of PC10, PC09, PC08 and PC07 represent 4.08, 4.16, 4.50, and 4.16 h. In Table 3, the adsorption capacities of PC10, PC09, PC08, and PC07 are 65, 66, 72 and 67 g/100 g. As compared with adsorption data com-
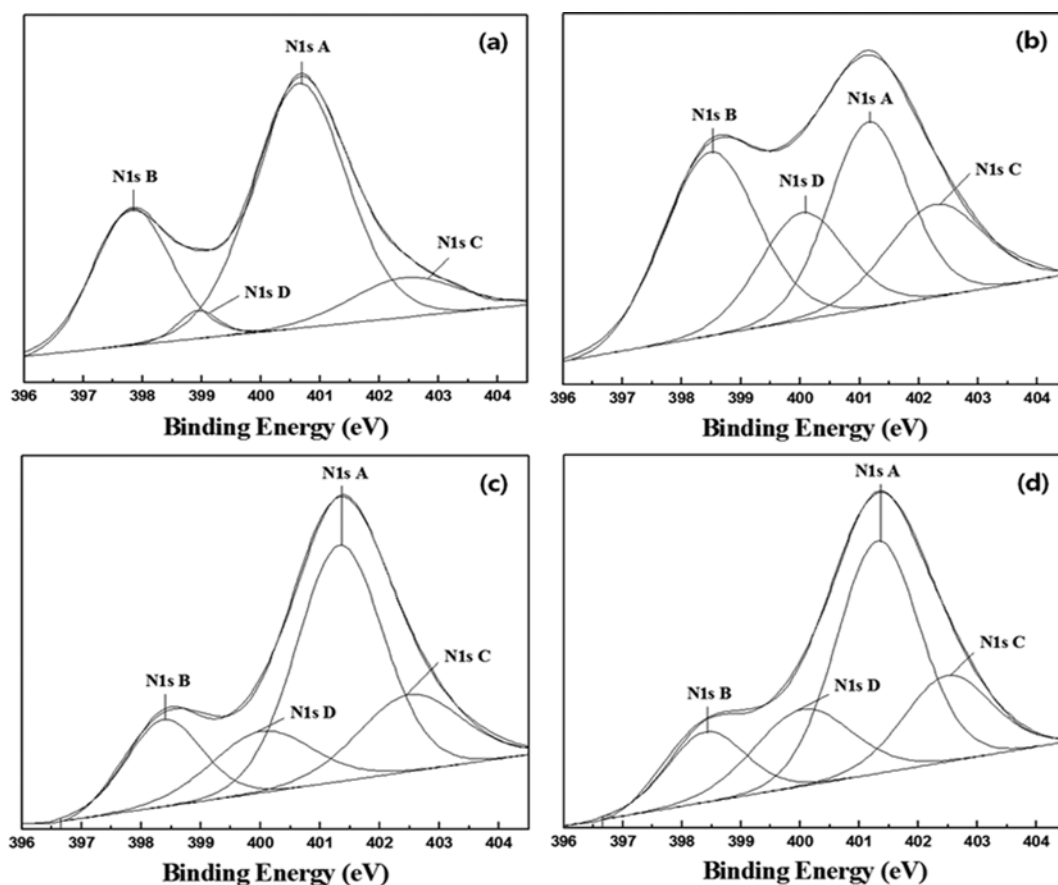
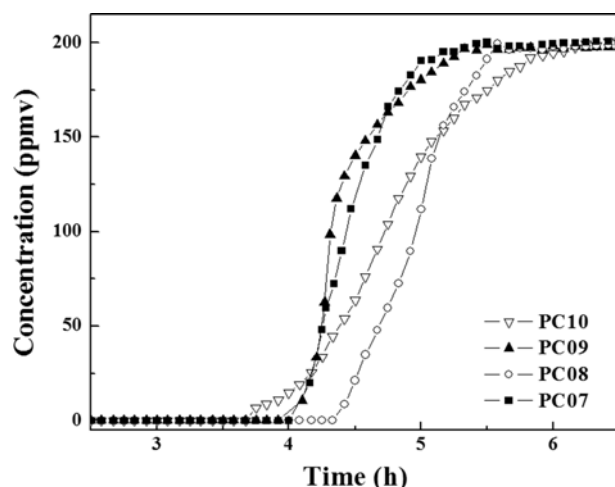**Fig. 7. N1s XPS spectra of (a) PC10, (b) PC09, (c) PC08 and (d) PC07.**

Fig. 8. Breakthrough curves of toluene adsorption.

Table 3. Breakthrough time and adsorption capacity

Sample	Breakthrough time (hr)	Breakthrough capacity (toluene-g/100 g)
PC10	4.08	65
PC09	4.16	66
PC08	4.50	72
PC07	4.16	67

piled from the literature by Lillo-Rodnas et al., these adsorption capacities are fairly remarkable [34]. The breakthrough time and adsorption capacity increased with CA content increasing up to 20% (PC08). This depends on the combination of the high specific surface area, appropriate average pore diameter, large micropore volume and surface chemistry characteristics. From the morphological point of view, it is natural that the higher surface area having high micropore volume results in a higher adsorption capacity and larger breakthrough time. To be sure, the average micropore diameters of blends are bigger than that of PC10, but it is still effective thinking from the molecular size of toluene. Moreover, steeper breakthrough curves were obtained for all blends than that of PC10. So, it is suggested that blended ACNFs have smaller mass transfer resistance and transfer area, and thus have good characteristics in kinetics and efficiencies.

CONCLUSIONS

Activated carbon nanofibers were prepared with polymer blends consisting of polyacrylonitrile (PAN) and cellulose acetate (CA), by electrospinning and subsequent thermal treatment. The average fiber diameter of samples was about 200 nm, ranging from 150 to 400 nm. The specific surface area, total pore volume, and micropore volume increased with increasing CA content. Pore characteristics for the adsorption performance were enhanced with increasing CA content (up to 20%). However, excess CA content (over 30%) was harmful to VOC adsorption ability due to changing the morphology of activated carbon nanofibers. The O/C ratio was in-

creased with increasing CA content. However, the O/C ratios of all activated carbon nanofibers prepared with blends represent small values, revealing non-polarity of the surface. The adsorption capacities of PC10, PC09, PC08 and PC07 were 65 g/100 g, 66 g/100 g, 72 g/100 g and 67 g/100 g, respectively. The blends of the PAN with CA showed better characteristics than those of PAN along, but apparently there is appropriate blending ratio (20%) for high-performance of activated carbonaceous materials.

REFERENCES

1. P. Dwivedi, V. Gaur, A. Sharma and N. Verma, *Sep. Purif. Technol.*, **39**, 23 (2004).
2. K. Na, *J. Environ. Manage.*, **81**, 392 (2006).
3. K. H. Chang, T. F. Chen and H. C. Huang, *Sci. Total Environ.*, **346**, 184 (2005).
4. S. D. Maleknia, T. L. Bell and M. A. Adams, *Int. J. Mass Spectrom.*, **262**, 203 (2007).
5. A. Ribes, G. Carrera, E. Gallego, X. Roca, M. J. Berenguer and X. Guardino, *J. Chromatogr. A*, **1140**, 44 (2007).
6. M. G. Evtyugina, C. Pio, T. Nunes, P. G. Pinho and C. S. Costa, *Atmos. Environ.*, **41**, 2171 (2007).
7. M. F. Mohamed, D. Kang and V. P. Aneja, *Chemosphere*, **47**, 863 (2002).
8. H. P. Kuo, S. W. Yao, A. N. Huang and W. Y. Hsu, *Korean J. Chem. Eng.*, **34**, 73 (2017).
9. A. Tarjomannejad, A. Farzi, A. Niaei and D. Salari, *Korean J. Chem. Eng.*, **33**, 2628 (2017).
10. Z. Guo, J. C. S. Chang, L. E. Spark and R. C. Fortmann, *Atmos. Environ.*, **33**, 1205 (1999).
11. A. L. Hinwood and P. N. Di Marco, *Toxicology*, **181-182**, 361 (2002).
12. A. Indarto, D. R. Yang, C. H. Azhari, W. H. W. Mohtar, J. W. Choi, H. Lee and H. K. Song, *Chem. Eng. J.*, **131**, 1 (2007).
13. K. J. Kim, C. S. Kang, Y. J. You, M. C. Chung, M. W. Woo, W. J. Jeong, N. C. Park and H. G. Ahn, *Catal. Today*, **111**, 223 (2006).
14. C. L. Chuang, P. C. Chiang and E. E. Chang, *Chemosphere*, **53**, 17 (2003).
15. P. Pre, F. Delage, C. Faur-Brasquet and P. Le Cloirec, *Fuel Process. Technol.*, **77-78**, 345 (2002).
16. J. Machnikowski, P. Rutkowski and M. A. Diez, *J. Anal. Appl. Pyrol.*, **76**, 80 (2006).
17. E. Raymindo-Pinero, D. Cazorla-Amoros, A. Linares-Solano and J. Find, *Carbon*, **40**, 597 (2002).
18. B. Grzyb, J. Machnikowski, J. V. Weber and A. Koch, *J. Anal. Appl. Pyrol.*, **67**, 77 (2003).
19. S. H. Park, C. Kim, Y. I. Jeong, D. Y. Lim, Y. E. Lee and K. S. Yang, *Synthetic Met.*, **146**, 207 (2004).
20. R. T. Yang, Adsorbents: fundamentals and applications, A John Wiley & Sons, INC. Publication (2003).
21. F. Watanabe, Y. Korai, I. Mochida and Y. Nishimura, *Carbon*, **38**, 741 (2000).
22. V. E. Kalayci, P. K. Patra, Y. K. Kim, S. C. Ugbolue and S. B. War-

ner, *Polymer*, **46**, 7191 (2005).

23. H. Ono and A. Oya, *Carbon*, **44**, 682 (2006).

24. D. D. Edie, *Carbon*, **36**(4), 345 (1998).

25. J. M. Deitzel, J. Kleinmeyer, D. Harris and N. C. Beck Tan, *Polymer*, **42**, 261 (2001).

26. C. Kim, Y. O. Choi, W. J. Lee and K. S. Yang, *Electrochim. Acta*, **50**, 883 (2004).

27. K. S. Yang, Y. J. Yoon, M. S. Lee, W. J. Lee and J. H. Kim, *Carbon*, **40**, 897 (2002).

28. P. J. M. Carrott, M. M. L. Ribeiro Carrott and P. A. M. Mourao, *J. Anal. Appl. Pyrol.*, **75**, 120 (2006).

29. G.-Y. Oh, Y. W. Ju, M. Y. Kim, H. R. Jung, H. J. Kim and W. J. Lee, *Sci. Total Environ.*, **393**, 341 (2008).

30. C. Liu and R. Bai, *J. Membr. Sci.*, **279**, 336 (2006).

31. C. Brasquet and P. Le Cloirec, *Carbon*, **35**, 1307 (1997).

32. K. J. Edgar, C. M. Buchanan, J. S. Debenham, P. A. Rundquist, B. D. Seiler, M. C. helton and D. Tindall, *Prog. Polym. Sci.*, **26**, 1605 (2001).

33. T. J. Xue, M. A. McKinney and C. A. Wilkie, *Polym. Degrad. Stabil.*, **58**, 193 (1997).

34. M. A. Lillo-Rodenas, A. J. Fletcher, K. M. Thomas, D. Casorla-Amoros and A. Linares-Solano, *Carbon*, **44**, 1455 (2006).

35. T. Oshima, Y. Kogami, T. Miyata and T. Uragami, *J. Membr. Sci.*, **206**, 156 (2005).

36. E. Raymindo-Pinero, K. Kierzek, J. Machnikowski and F. Beguin, *Carbon*, **44**, 2498 (2006).

37. S. K. Ryu, B. J. Park and S. J. Park, *J. Colloid Interface Sci.*, **215**, 167 (1999).

38. Z. H. Huang, F. K. Kang, Y. P. Zheng and J. B. Yang, *Carbon*, **40**, 1363 (2002).

39. A. P. Terzyk, *Colloids Surf., A*, **177**, 23 (2001).